A KINETIC MODEL FOR THE ENERGY TRANSFER IN PHYCOBILISOMES

GEORG W. SUTER AND ALFRED R. HOLZWARTH
Max-Planck-Institut für Strahlenchemie, D-4330 Mülheim/Ruhr, Federal Republic of Germany

ABSTRACT A kinetic model for the energy transfer in phycobilisome (PBS) rods of *Synechococcus 6301* is presented, based on a set of experimental parameters from picosecond studies. It is shown that the enormous complexity of the kinetic system formed by 400–500 chromophores can be greatly simplified by using symmetry arguments. According to the model the transfer along the phycocyanin rods has to be taken into account in both directions, i.e., back and forth along the rods. The corresponding forward rate constants for single step energy transfer between trimeric disks are predicted to be 100–300 ns^{-1}. The model that best fits the experimental data is an asymmetric random walk along the rods with overall exciton kinetics that is essentially trap-limited. The transfer process from the sensitizing to the fluorescing C-PC phycocyanin chromophores ($\tau \approx 10$ ps) is localized in the hexamers. The transfer from the innermost phycocyanin trimer to the core is calculated to be in the range 36–44 ns^{-1}. These parameters lead to calculated overall rod–core transfer times of 102 and 124 ps for rods containing three and four hexamers, respectively. The model calculations confirm the previously suggested hypothesis that the energy transfer from the rods to the core is essentially described by one dominant exponential function. Extension of the model to heterogeneous PBS rods, i.e., PBS containing also phycoerythrin, is straightforward.

1. INTRODUCTION

Phycobilisomes (PBS)[1] are supramolecular light-harvesting antennae of cyanobacteria (blue-green algae) and red algae (1–9). They are attached to the outer surface of the thylakoid membrane of these organisms (10) and consist of aggregates of phycobiliproteins containing covalently bound tetrapyrrolic chromophores (11). All PBS contain a core of a pigment called allophycocyanin (APC) and, attached to it in a radial structure, rods consisting of stacked trimers or hexamers of either the same or different types of phycobiliproteins (3, 12). Perhaps the simplest type of PBS is that of the cyanobacterium *Synechococcus 6301* (S 6301, *Anacystis nidulans*) whose structure has been studied in much detail. The APC core consists of two disk-like structures from which radiate six cylinders, each composed of several hexameric disks (9, 13). Even simpler than the wild-type PBS are those of a mutant (AN 112) derived from S 6301. They contain only one hexameric disk of C-PC in each rod (13).

PBS are optimized for efficient energy transfer, which proceeds energetically "downhill" from the periphery to the core. In vivo, the PBS feed primarily the photosystem II reaction centers (14, 15). The energy transfer kinetics in PBS and their constituent phycobiliproteins have been studied extensively recently (for reviews see references 16–18). It has been found that the transfer proceeds on a picosecond time scale, generally requiring between 50 and 150 ps only to pass the energy from the periphery of the PBS to the final emitter APC B. The picosecond studies revealed many details of the energy transfer processes in PBS. In particular the transfer kinetics between the pigment beds of the different types of phycobiliproteins could be studied, as well as the transfer from the sensitizing "S"- to the fluorescing "F"-chromophores, either within an individual phycobiliprotein in the isolated form, or as part of a PBS (19–25). However, other important aspects like, e.g., the transfer processes between identical or nearly identical pigments (homotransfer) and the related single step transfer times in PBS, cannot be studied directly. Unless we obtain information on these "hidden parameters" a full understanding of the energy transfer processes in PBS rods cannot be attained.

Attempts have been made to gain more insight into these processes by looking at the anisotropy decay in PBS by either fluorescence or transient absorption (21, 23, 26, 27). It has been found that upon excitation with polarized light the anisotropy decays rapidly on the time scale of a few tens of picoseconds (21, 23, 27–30). However, these studies, besides proving the occurrence of very fast homo- and heterotransfers, did not yield very detailed information on the single step transfer processes and the flow of the energy. This was partly due to a deficiency in information on the relative orientation of the chromophores and to the lack of an adequate theory to describe the anisotropy decay

[1] *Abbreviations used in this paper:* APC, allophycocyanin; C-PC, C-phycocyanin; F, fluorescing chromophore; M, intermediate chromophore; PBS, phycobilisome(s); PE, phycoerythrin; S, sensitizing chromophore.

Correspondence should be addressed to Dr. Holzwarth.

function in the case of energy transfer. The detailed structure information that became recently available for C-phycocyanin (C-PC) (31) is expected to change this situation profoundly (32–34). It should be kept in mind, however, that the exact orientation of the transition dipole moments that is required for theoretical calculations of energy transfer kinetics cannot be obtained exclusively from the x-ray analysis. In view of this situation, a kinetic model of the energy transfer that uses the experimental data known so far would, even if it had to make simplifying assumptions, reveal some of the "hidden" parameters and thus give more insight into the details of the transfer processes involved. In particular, such a model should be suitable for clarifying whether, and under which conditions, a relatively simple description of the transfer kinetics by only a small number of exponentials may be valid. It could also provide a basis for distinguishing between $\exp(-t^{1/2})$ kinetics and a sum of exponentials model (35, 36). The latter kinetics is strongly suggested by our experimental data (37).

We have recently studied the energy transfer kinetics in a "simple" PBS and some of its constituent phycobiliproteins using various technique (20, 23, 24, 30, 37). These data provide the basis for the quantitative kinetic models presented in this work. Starting from a fairly simple model, more complexity will be added to arrive finally at a model sophisticated enough to allow an adequate description of the energy transfer processes in the simple PBS from *Synechococcus 6301*. There is very little quantitative information available so far on the energy transfer processes within the PBS cores (23, 38). For this reason we do not describe these processes in detail in this work. Instead we concentrate on the homogeneous PBS rods. For comparison, and without going into details, these results will finally be extended to heterogeneous PBS rods, i.e., to PBS rods containing also phycoerythrin.

2. THE PBS MODELS

a. Experimental Basis of the PBS Models

The experimental data obtained from picosecond measurements on isolated PBS from *Synechococcus 6301* (20, 30), the mutant AN 112 (23), and isolated C-PC in various aggregation states (24, 25, 37) are described in detail in these references. The most pertinent data are collected in Table I. The experimental overall rod → core transfer times (corresponding to the main decay component of C-PC emission and the rise of APC emission) found in PBS of different rod lengths as well as the S → F transfer times provide the calibration points for our model. These data are complemented by results obtained from measurements on red algal PBS which, in addition to one hexameric unit of phycocyanin, contain also phycoerythrin in their rods (21, 22, 39).

b. Different PBS Models

All PBS models used in this work consist of an APC core whose fine structure is not further specified. It is assumed that it contains near the rod attachment site identical APC chromophores (identical in the sense of equal spectra and kinetic behavior), which act as a trap for the energy transferred from the rods. Attached to this core are six identical PBS rods composed of two to eight trimers (or one to four hexamers) of C-PC. The transfer kinetics, in particular the transfer from the rods to the core, is assumed to be identical for each of the six rods.

Förster transfer (40, 41) is generally assumed to be the mechanism by which energy is transferred between chromophores in PBS. This assumption is strongly supported by recent calculations of Förster energy transfer rates in C-PC by Sauer and Scheer (32) based on the x-ray structure (42). The results of this study are in fairly good agreement with our experimental data (24). We should like to point out, however, that the conclusions drawn in this work are of a general nature and do not necessarily require a Förster mechanism for energy transfer although this mechanism is the most likely one.

The following general assumptions are made in our model: (*a*) The energy transfer between trimers that are not neighbors can be neglected due to the R^{-6} (in the case of a Förster mechanism) or some other distance dependence of the transfer rates. (*b*) Back-transfer from the core to the rods is excluded partly due to the small spectral overlap factor for such steps and partly because the initial

TABLE I
ENERGY TRANSFER PARAMETERS OBSERVED IN C-PHYCOCYANIN AGGREGATES (A) AND IN PBS OF *SYNECHOCOCCUS 6301* OR THE MUTANT AN 112 (B)

A C-PC aggregates*	Monomeric	Trimeric	Hexameric	PBS rods
S → F transfer	46 ps	22‡ ps	10 ps	10–15 ps
Reference	(24)	(24, 25)	(23)	(30)
B PBS				
Hexameric units per rod		1	3	4
Overall rod → core transfer		45 ps§	83 ps	120–130 ps§
Reference		(23)	(23, 30)	(20)

*See also reference 24.
‡35 ps for trimers without linker protein (25).
§Equivalent to the experimental APC emission rise time.

transfer to APC is followed by additional fast transfer steps to APC-B and/or the colored linker peptide, which both quickly depopulate the APC chromophores (38, 43). (*c*) There is a threefold symmetry axis along the C-PC rods (31, 42). This symmetry is assumed to hold also for the direct rod–core transfer, i.e., the symmetrically equivalent C-PC chromophores of the innermost trimer are assumed to have identical transfer rates to the core. (*d*) The spectral properties of the C-PC trimers/hexamers are considered to be independent of their distance to the core. Nevertheless, different rate constants for transfer back and forth along the rods are taken into account by choosing an appropriate *f*-factor (for further discussion see below). (*e*) The radiative lifetime of C-PC and APC is assumed to be 6 ns (44). (*f*) The observed fluorescence lifetime in the absence of energy transfer is ≈1.8 ns for C-PC and APC (20, 23, 24).

In the simple basic model A all C-PC chromophores within a trimer are treated as being identical, i.e., no distinction (neither spectral nor with respect to kinetic parameters) is made between the three types of C-PC chromophores: S (sensitizing), M (intermediate), and F (fluorescing) (24, 45, 46). Furthermore, the energy transfer rate constant from one trimer to its neighbor is assumed to depend only on the direction of transfer (i.e., towards the core or away from it) but not on the distance of the trimers from the core.

Model B is basically identical to A but now hexamers are taken as the basic units building the C-PC rods instead of trimers.

Model C describes both the transfers along the rods as studied in models A and B as well as the transfers between the different C-PC chromophores (S, M, and F). Their spectral differences are now taken into account explicitly. According to the results obtained from studying model B (cf. Section 4.3) the basic units of this model are trimers. The spectra of the individual chromophores used for the model calculations have been taken from reference 46 and are shown in Fig. 1 (see also reference 24). The APC spectra have been taken from reference 13.

3. RESULTS AND DISCUSSION

3.1 Model A

This model was used as a starting point. It serves merely to elucidate the general conditions that have to be fullfilled for the rate constants of the transfer along the C-PC rods and the rod → core transfer to match the experimental data qualitatively. The spectral differences between sensitizing and fluorescing chromophores were not taken into account, and all C-PC chromophores in a trimer were assumed to be symmetrically equivalent. The long-lived contribution of the APC emission was neglected.

The following parameters are introduced to describe the energy transfer kinetics in this model (Fig. 2 *a*): (*a*) k_{RC}, the rate constant for the energy transfer from the C-PC

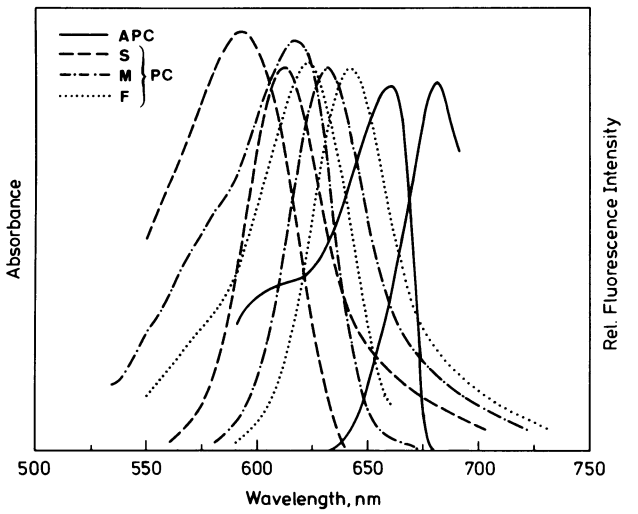

FIGURE 1 The model fluorescence and absorption spectra of the phycobiliproteins C-PC and APC used in the model calculations shown in Fig. 6 (taken from references 46 and 13).

chromophores of the trimer closest to the core to the APC chromophores in the core. (*b*) k_{RR}, the rate constant for the energy transfer from C-PC chromophores in one trimer to the nearest neighbor trimer in a direction towards the core.

Note that these *k* values are actually the sums of the rate constants of transfer processes starting on a particular chromophore and leading to the group of symmetrically equivalent acceptor chromophores (see Appendix). (*c*) *f*, the ratio between corresponding rate constants inside the rods valid for transfers away from (k_{distal}) and toward ($k_{proximal}$) the core, respectively (see Fig. 2 *a*):

$$f = k_{distal}/k_{proximal}.$$

It is important to note that the relative contribution of the different transfer paths starting from a particular chromophore in one trimer and leading to the chromophores in a

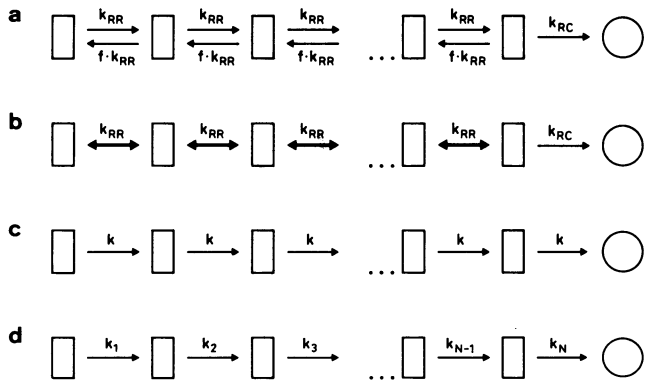

FIGURE 2 Kinetic schemes for model A and some limiting cases. (*a*) Standard model. k_{RC}, rod–core transfer rate; k_{RR}, transfer rate from one trimer to its neighbor towards the core; *f*, factor for back-transfer along the rod. (*b*) $f = 1$, $k_{RR} \gg k_{RC}$. (*c*) $f = 0$, $k_{RR} = k_{RC} = k$. (*d*) $f = 0$, k_{RR} slightly dependent on the distance from the core, $k_{RC} = k_N$.

neighboring trimer is not relevant in this model, as long as the respective acceptor chromophores are symmetrically equivalent in that trimer and as long as the sum of all these transfer rate constants is conserved (see Appendix). For simplicity of calculation we have assumed identical spectra for the trimers, independent of their position in the rod. However, this simplification could be removed in the calculation if it would seem to be appropriate. The f-factor allows us nevertheless to take into account the known position dependence of the trimer spectra (13). This position dependence of the spectra gives rise to different overlap factors for Förster transfer and thus leads to an asymmetry, i.e., a direction dependence, of energy transfer rate constants for transfer along the rods. Taking into account this asymmetry is of fundamental importance in modeling the PBS transfer kinetics.

It was assumed that the experimentally observed rise time of the APC fluorescence, which in our experiments was always identical with the observed main decay time of C-PC fluorescence (20, 23, 30), must be correlated with the longest-lived rod → core energy transfer component (designated τ^*) predicted by the model. This correlation is appropriate because the amplitude of this longest-lived transfer component is always predicted to be the largest one in the model kinetics. Moreover, still longer transfer times would have been easily detected as rising terms of the APC emission in the experiment, whereas the very short-lived (<5 ps) components, also predicted by the model under certain conditions, are difficult to observe experimentally so far.

The calculated decay function generally is simpler for f factors close to 1. In this case the longest-lived decay component clearly dominates the decay, whereas for small f factors the decay becomes essentially multiexponential for long rods (three to four hexamers per rod). With increasing rod length the predicted longest-lived rod → core transfer component τ^* increases more steeply for large f factors than for small ones (cf. Fig. 4). These features may be understood by looking at two limiting cases, which still allow an analytical treatment: (*i*) ($f = 1$; $k_{RR} \gg k_{RC}$; this is the case of symmetrical back transfer within the rods (deactivation processes other than energy transfer are assumed negligible) (Fig. 2 *b*). In this case, which corresponds to a trap-limited symmetric random walk along a one-dimensional array (47), the decay function of all trimers is identical due to the fast and symmetric transfer within the rod. Thus the decay of excited states in the rod is monoexponential with an overall decay time of

$$\tau_{obs} = N \cdot (1/k_{RC}),$$

i.e., $\tau^* = \tau_{obs}$ increases linearly with N, the number of trimers per rod. Decreasing k_{RR} increases the τ^* values for $N > 1$. Thus, in all models with f values close to 1, the main component τ^* will increase too steeply with N as compared with the experimental data (Table I B).

On the other hand, with $k_{RC} \gg k_{RR}$ one obtains a diffusion-limited transfer. In this case the average number of transfer steps within a rod before final trapping in the core occurs is $\langle n \rangle = N(n + 1)/6$ for a symmetric random walk along a one-dimensional array (48, 49). The resulting decay function is very complex (47), but the overall rod → core transfer time will increase proportionally to $N(N + 1)$. Comparison with the experimental data (Table I B) reveals that a functional dependence of the type $\tau^* \approx N^\alpha$ is required, with $\alpha < 1$. Thus, neither the extreme trap-limited nor the diffusion-limited random walk model with symmetrical transfer along the rods provides an adequate description of the observed PBS kinetics. (*ii*) $f = 0$; $k_{RR} = k_{RC} = k$; this is the limiting case of unidirectional transfer, i.e., no back transfer within the rods is allowed (deactivation processes other than energy transfer are assumed to be negligible).

These conditions (Fig. 2 *c*) lead to degenerate eigenvalues of the corresponding kinetic matrix. This model was implicit in the analysis of the PBS kinetics by Glazer et al. (50). The decay function $d(N, t)$ of the excitons in the rods can be solved analytically. It is given by

$$d(N, t) = \sum_{v=0}^{N-1} \frac{N - v}{v!} \cdot k \cdot t^v \cdot \exp - kt,$$

which is not longer simply a sum of exponentials. The first moment of this decay (mean lifetime τ_m) increases linearly with N, the number of trimers in the rod:

$$\tau_m = \frac{\int t \cdot d(N, t)dt}{\int d(N, t)dt} = 1/k \cdot \frac{(N + 2)}{3}.$$

However, it is important to note that τ_m is not an exponential lifetime.

Purely exponential decay times may be obtained by considering a similar model with no back transfer ($f = 0$) but with slightly different rate constants for the transfer steps between the individual trimers (Fig. 2 *d*). In this model the degeneracy met above will be removed and the decay function for rods with N trimers may be described as follows:

$$d(N, t) \propto \sum_{i=1}^{N} x_i(t),$$

where $x_i(t)$ is the concentration of PBS carrying an excited chromophore in trimer i ($i = 1$ for the outermost trimer)

$$x_i(t) = e^{-k_i t} + k_{i-1} \int_{t'=0}^{t} x_{i-1}(t') e^{-k_i(t-t')} dt'.$$

The first term represents the decay initiated by direct excitation of the trimer i. The second term results from the excitation of the trimer i from the trimer $(i - 1)$ by energy transfer. Since $x_1(t) \propto e^{-k_1 t}$, it follows that $x_i(t)$ may be written as

$$x_i(t) = \sum_{m=1}^{i} a_{im} e^{-k_m t}.$$

The coefficients a_{im} may be expressed recursively by calculating the convolution integral and comparing the coefficients on both sides of the equation:

$$a_{im} = a_{(i-1)m} \frac{k_{(i-1)}}{\Delta_{im}} \qquad m = 1 \ldots (i-1)$$

$$a_{ii} = 1 - \sum_{m=1}^{i-1} a_{im}$$

$$a_{11} = 1,$$

where k_j is the transfer rate from the trimer j to the trimer $(j+1)$, k_N is the rod–core transfer rate constant, and Δ_{im} is $k_i - k_m$.

It appears that such a model leads to a very complex multiexponential decay. The decay constants k_j of the various components are those of the individual transfer steps between trimers. Therefore in this model only the number of exponentials, and thus the complexity of the decay function but not the decay times themselves, increases with the number of trimers per rod. Such a kinetic behavior would not be in agreement with the experimental results, which indicate a significant increase in the lifetime of the main component of energy transfer with rod length. Also a large number of significant terms with negative amplitudes are predicted by this model, but have not been found in the measurements. Thus, based on these considerations, both limiting cases, i.e., $f \rightarrow 0$, and $f \rightarrow 1$, may be ruled out. Having investigated these limiting cases, we are now ready to carry out more detailed numerical simulations.

3.2 Numerical Calculations

The decay function of the rod emission was calculated numerically using the formalism developed in the Appendix, for different sets of fixed values for f and k_{RC} (see Fig. 2 *a*). The results of these fits are shown in Figs. 3 and 4. k_{RR} was optimized for each pair of the fixed parameters such that the lifetime of the predicted longest-lived transfer component fitted best the experimental values for the observed rod → core transfer listed in Table I B. The mean relative deviation (MRD) was taken as the measure for the goodness of fit, which is equivalent to the assumption that all experimental values have the same relative error.

$$\text{MRD} = (1/3) \cdot \sum_i \left(\frac{\text{Calculated} - \text{Experimental}}{\text{Experimental}} \right)^2.$$

The diagrams in Fig. 4 show the calculated amplitudes and decay times obtained for emission from the rods for various fixed f factors and the corresponding best fit values of k_{RR} and k_{RC}. For f values lower than 0.9, the best MRD value does not change significantly. For $f = 1$ this value increases drastically, indicating poor agreement of the calculated τ^* values with the experimental data. This was already expected from the analytical considerations discussed above. Even more conclusive are the unrealistically high k_{RR} values required for an optimum fit in cases where f is larger than ~0.75 (cf. Fig. 3).

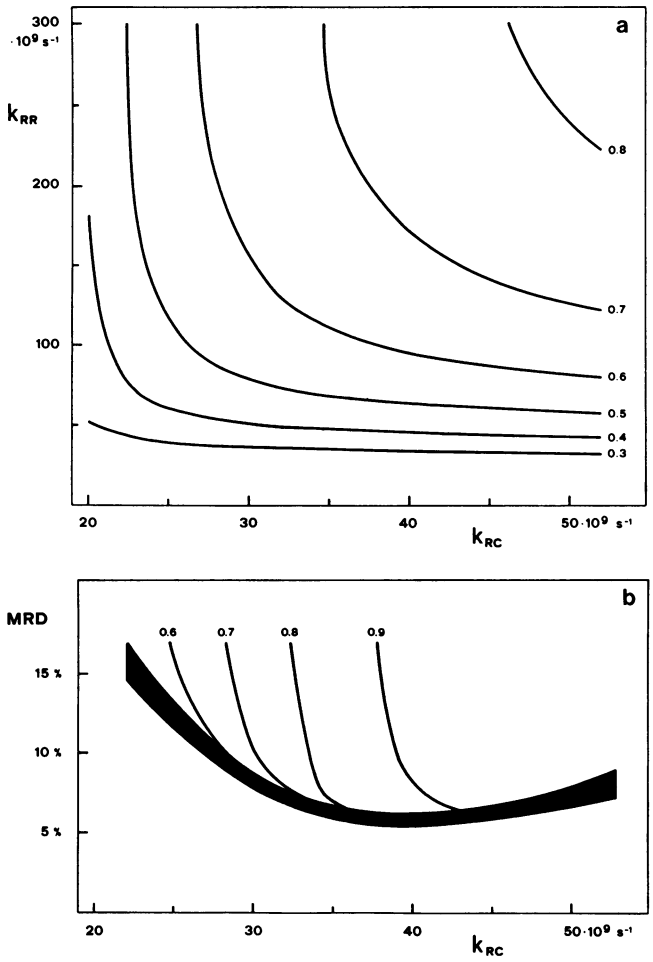

FIGURE 3 Rate constants k_{RR} for transfer along the rods (*a*) and deviations MRD (*b*) obtained from fitting the calculated main component for rod → core transfer τ^* (see text) to the experimental data given in Table I with model A. The values of k_{RC} and f were fixed for the individual fits. The best-fit k_{RR} values increase with increasing f values. The minimum MRD value does not change significantly for f values ≤0.8. The MRD curves for $f = 0.3$, 0.4, and 0.5 lie within the black band. The optimum k_{RC} value is 40 ± 4 ns^{-1} for all f values ≤0.7 and increases for larger f values.

The Förster radius R_0 (for randomly oriented chromophores) for C-PC → C-PC transfer is between 47 (51) and 56 Å (30). Assuming an average distance of 30 Å (i.e., approximately the thickness of a C-PC trimer) between two chromophores in different trimers involved in the transfer along the rod(s), the corresponding pairwise single step transfer rates should, even in the case of optimum relative orientation, not exceed values of ~300 ns^{-1}.

In our model A there are nine potential acceptors in the neighboring trimer for a given excited chromophore. From the crystal data (31) and the approximate Förster radii given above, it may be estimated that not all of them are efficient acceptors but only perhaps between three and six of them. We thus estimate an upper limit for the total K_{RR}

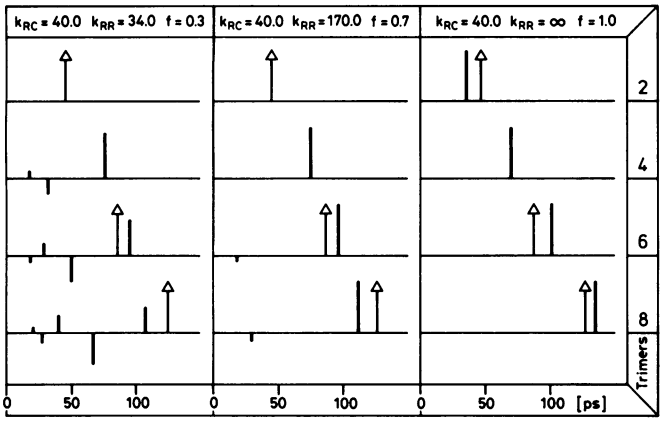

FIGURE 4 The optimized decay components of the rod emission in model A for different f values. The length of the bars (positive up and negative down) indicates amplitudes, while the associated lifetimes are given by the position on the abscissa. The experimental calibration points (cf. Table I) are marked with triangles. Note that the lifetime of the main component increases more steeply with increasing rod length for large as compared with small values of f. Moreover the decay is more complex for small f values.

of ~1,000 ns^{-1} (note that this is the sum of the pairwise single step rate constants).

The decay functions for $f \leq 0.5$ do not show a single dominating component. They are rather composed of a multitude of exponential functions with comparable amplitudes. Moreover there are significant components with negative amplitudes (rising terms), which are not found in the experimental data. Simulations have shown that such rising terms would have been revealed by the data fitting procedures used in investigations of the PBS kinetics (20, 23). For these reasons $f \leq 0.5$ can be excluded.

In summary, a model of type A is consistent with the experimental data if f is ~ 0.6–0.7 and k_{RC} and k_{RR} are in the range of 40 ± 4 ns^{-1} and 100–300 ns^{-1} (note that the latter are single step rate constants), respectively (see Fig. 4, *middle*). Such an intermediate value for f appears to be in agreement with the known rod asymmetry, i.e., the red shifts in the spectra of the C-PC units, which are closer to the core (13). This red-shift is responsible for a smaller overlap factor for Förster transfer in the direction away from the core as compared with the direction towards the core.

The model A can also be easily extended to fluorescence kinetics of heterogeneous rods, i.e., to PBS containing also phycoerythrin (PE) (21). For a rod length of six trimers (the four outer representing PE, the two inner ones C-PC) and using the same kinetic parameters as above, except that the transfer between the adjacent PE- and the C-PC trimer is assumed to be irreversible, the model yields the following decay functions upon selective excitation of the PE-chromophores:

$$d(PE, t) \simeq 0.95 \cdot \exp(-t/36\ ps) + \text{terms with amplitudes} < 0.05 \quad \text{(phycoerythrin decay)}$$

$$d(PC, t) \simeq 1.00 \cdot \exp(-t/41\ ps) - 0.99 \cdot \exp(-t/36\ ps) - \text{terms with amplitudes} < 0.01 \quad \text{(phycocyanin rise and decay).}$$

These values are in good agreement with the transfer kinetics that have been observed, e.g., in PBS of *Porphyridium cruentum* (21, 22).

4.3 Model B

Both the protein structure determined by x-ray analysis (42) and the fine structure appearing in electron micrographs (13) of PBS indicate that the basic unit of the PBS rods is the hexamer of C-PC. This is also supported by spectroscopic data: The S → F transfer rate observed in C-PC hexamers (24) is identical to that in intact PBS (37). One should notice that the hexamers consist of two trimers in a head-to-head configuration (42). Such hexamers should be fully symmetric with respect to transfers between the constituent trimers. However, to fit the observed C-PC depletion kinetics of PBS with rods built up of such symmetrical hexamers, the asymmetry factor f for the transfer between the hexamers has to be reduced below 0.5, which again leads to complicated decays with many positive and negative components (see above). Higher f values would lead to better agreement but would require exceedingly high transfer rates within the hexamers, which are unlikely in view of the estimated maximum rate of 1,000 ns^{-1} (see above). Another consequence of such a model would be that the intrahexamer transfer rates between trimers would be drastically different from the interhexamer transfer rates. It cannot be ruled out of course that isolated hexamers are to a good approximation symmetric with respect to transfers between the trimers (see next section), but become asymmetric upon rod formation. In view of these difficulties we presently feel that a PBS kinetic model assuming large differences between interhexamer and intrahexamer transfer rates between trimers (model B) to be less appropriate than a model where these rates are more equal (model C). Setting these rates equal actually is equivalent to a model where the basic units for energy transfer along the rods are the trimers.

4.4 Model C

For the reasons discussed above we have chosen to calculate this model in the most detail. In this model the different spectral properties of the three types of C-PC chromophores are taken into account explicitly. The experimental results along with a detailed kinetic model for the energy transfer processes within isolated C-PC aggregates have been presented in reference 24.

We now build up rods from trimers. The kinetic parameters for the S → F transfers between two neighboring trimers will be chosen such that the resulting kinetics of

transfer between chromophores of a hexamer in the rod is the same as that observed in the isolated hexamers (24). This is consistent with the equal rate constant of S → F transfer kinetics for isolated hexameric C-PC units and intact PBS (see Table I) (23, 24, 37). For conceptual simplicity we assume that the transfer along the rod occurs essentially between chromophores of the same type only, i.e., S → S, M → M, and particularly F → F. This seems justified in view of the x-ray data of C-PC, which indicate that in particular the β-84 chromophores but also the α-84 chromophores are closely parallel with their transition dipole moments in the two trimers forming a hexamer and probably also for interhexamer transfer (42). It is important also that under this assumption the S → F transfer kinetics established experimentally in the isolated hexamer are not affected in the PBS (see above). The relevant transfer processes for this model are depicted schematically in Fig. 5.

Details of the mathematical procedures used to numerically solve the kinetic equations for energy transfer kinetics in the PBS rods are discussed in Appendix A. Using this formalism we have calculated the time-resolved spectra for PBS rods of four hexamers (eight trimers) corresponding to the model shown in Fig. 5. The model kinetic parameters were taken from the optimization of model A on the one hand and the hexamer model presented in reference 24 on the other hand (see also Table I). The diagram in Fig. 6 shows the results, which are in good qualitative and reasonably quantitative agreement with the experimental findings (20, 23). The total number of relevant kinetic components is surprisingly low. Only one kinetic component dominates the overall rod → core transfer. (Three very fast exponential components with lifetime $\tau < 8$ ps and relative amplitudes <5% over the whole spectrum were omitted.) The calculated decay components may be easily

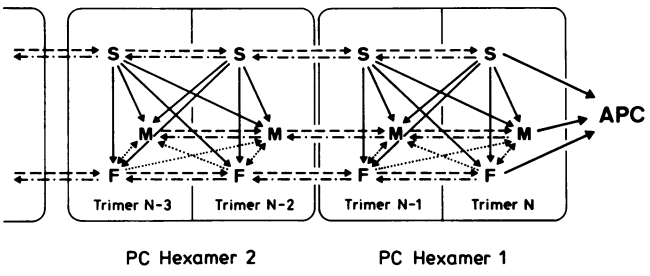

FIGURE 5 The PBS model C used in the calculation of the time-resolved spectra shown in Fig. 6. Only two hexamers are shown. The following parameters are applied: k_{RC}, 44 ns^{-1} (→); k_{RR}, 150 ns^{-1} (- - -); $f \cdot k_{RR}$, 105 ns^{-1} (back-transfer along the rod) (-.-.-); k_{SM}, 22 (28) ns^{-1} (→); k_{SF}, 22 (28) ns^{-1} (→); k_{MF}, 3 (12) ns^{-1} (.....); k_{FM}, 2 (3) ns^{-1} (....). The values in parentheses refer to transfers between chromophores of the same trimer. Note that only the sums $k_{SM} + k_{SF}$ and $k_{MF} + k_{FM}$ are observable in the experiment, i.e., any combination of individual parameters that leaves these sums constant is, within the model, consistent with the experiment. However, to observe the longer ps component, k_{MF} and k_{FM} must be different. The parameters are chosen based on the calculations for model A and according to the data from the hexamer model presented in reference 24.

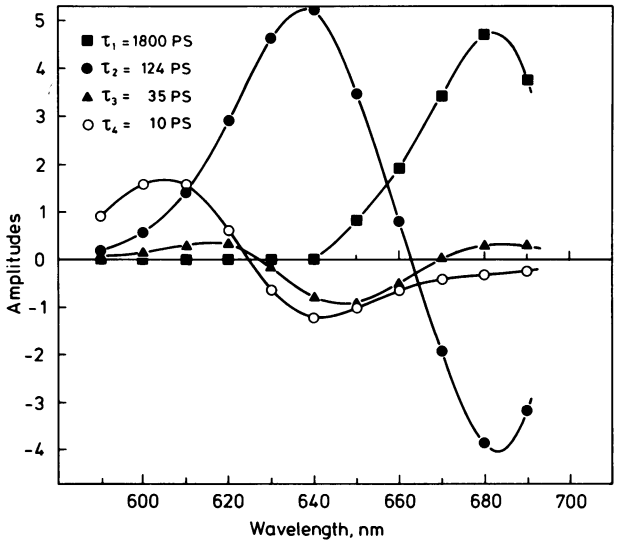

FIGURE 6 Calculated fluorescence decay components (amplitudes) as a function of emission wavelength resulting from the PBS model C (Fig. 5) for rods of four hexamers and an assumed excitation wavelength λ_{ex} = 590 nm. Three components having relative amplitudes of <5% at their maximum have been omitted. Two components with similar lifetimes (30 and 38 ps) are combined to the 35-ps component. These data should be compared with the experimental results given in references 20, 23, and 37 and Table I.

understood in terms of transfer processes met already in the simpler models:

1.8 ns, APC emission

124 ps, overall rod-core transfer (C-PC depletion) for four hexamers; (largest amplitude in the C-PC emission region, equivalent to the rise time for the APC emission; this component corresponds to the τ^* component referred to in the text)

38 ps*, M ↔ F transfer

30 ps*, negative term of the rod-core transfer (cf. Section 4.1)

10 ps, fast depletion of S-chromophore(s).

The two components with a superscript asterisk have been combined to the "35-ps component" in Fig. 6. All decay components predicted by this model have been found experimentally in PBS fluorescence, except for the ≈35-ps components, which have a small amplitude. Also the rising (negative amplitude) part of the 10-ps component has not been found so far. These components will be difficult to detect experimentally. However, a complete time-resolved spectrum analyzed with the global analysis procedure, analogous to the time-resolved spectra of C-PC (24), might allow to reveal these components. This would provide an even more stringent check of the proposed kinetic model than has been possible so far. Experimental work along this line is in progress.

It has been claimed that the fluorescence decay kinetics of PBS can be described by a nonexponential (exp $- k\sqrt{t}$) decay law (35, 36, 52, 53). In some cases in fact parts of

the experimental decay may be described equally well with a double exponential or with a exp $(-k\sqrt{t})$ decay function (39), in particular when the signal-to-noise ratio is low. If, however, the time-resolved spectra are considered, a hidden exp $(-k\sqrt{t})$ component should appear as two (or more) exponential components with amplitudes that show the same dependence on wavelength. This has never been observed so far (20–24, 37) and is also not supported by the model calculations presented here. One should, on the other hand, be aware of the fact that in cases where the energy transfer involves many nearly irreversible steps in the light harvesting system (i.e., $f \rightarrow 0$), such "pairs" of exponentials, with identical spectral distribution, may occur even if no exp $(-k\sqrt{t})$ kinetics is present.

CONCLUSIONS

We have developed a detailed kinetic model for the energy transfer in the PBS rods of the homogeneous, i.e., phycocyanin-containing PBS of *Synechococcus* and its mutant AN 112. The kinetics for rod-to-core transfer is described by the sum of a small number of exponential terms. This finding and the predicted wavelength dependence of the amplitudes of these components are in agreement with our previous experimental findings. The kinetic model predicts that the rate constant for transfer from the innermost trimer to the core with a rate constant of 40 ns^{-1} is rate-limiting for the overall transfer.

The model also predicts that the transfer rates along the rod between trimers and/or hexamers are extremely fast, occurring with pairwise single step rate constants of 100–300 ns^{-1}. They are thus much faster than the transfer steps within a single trimer or hexamer. The transfer along the rod between the C-PC aggregates is largely reversible. We get best agreement with the experimental data with an asymmetry factor $f \approx 0.7$. This is the ratio of the backward to forward transfer constants along the rods. We have also estimated this asymmetry factor from the overlap integral of the spectra of C-PC with different linker peptides given in reference 13. The calculated asymmetry factors are in the range of 0.6–0.7, depending on the specific pair of phycocyanins. The agreement with our optimum fit value in the kinetic model of $f \approx 0.7$ is therefore satisfactory.

We conclude that the kinetic model presented allows a fairly detailed determination of those hidden kinetic parameters in the PBS kinetics, which cannot be determined directly by kinetic measurements. The transfer steps between trimeric and/or hexameric disks within a rod are predicted to be the fastest transfer steps in the whole PBS. This trap-limited transfer predicted by our model is therefore in contrast to recent suggestions that the transfer along the rods should be limited by disk-to-disk transfer (50). The latter would be a diffusion-limited kinetics. Our results show that such a model would result in a much more complex transfer kinetics than is found experimentally.

The extremely fast transfer along the rods predicted by our calculations requires a highly favorable orientation of the chromophores involved. From the structural point of view the best candidates for the transfer along the rods seem to be the $\beta = 84$ and also the $\alpha = 84$ chromophores (31, 42). The partial conservation of the polarization anisotropy during transfer along the rods provides good experimental evidence for this predominant transfer path along the rods between nearly parallel oriented chromophores (21, 23, 30).

APPENDIX A

The Mathematical Basis

The kinetic problem is described by a series of first order differential equations. These equations are solved using appropriate boundary conditions, i.e., initial excitations described by weighting factors that are determined by the spectral shape of the absorption and emission of the individual pigments. Symmetry arguments are used to simplify the complexity of the problem.

Consider $\mathbf{X}_{mn}$ as the concentration vector of PBS carrying an excited X-chromophore in the nth trimer (the first trimer being the outermost) at position m ($n = 1, \ldots, N$; $m = 1, 2, 3$; $X = $ S, M, F, and APC) one obtains $3 \times 3 \times N + 1$ differently excited PBS. (Remember that the six rods are treated as identical and that the APC core is considered as one single terminal "superchromophore" acting as a trap.)

Collecting the X_{mn} in the vector $\mathbf{X}$, the system of differential equations describing the kinetics is

$$\partial \mathbf{X}/\partial t = K \cdot \mathbf{X},$$

where K is a matrix of all rate constants. The groups of symmetrically equivalent chromophores lead to the rather simple structure of K, which is dominated by the 9×9 blocks related to the nine chromophores in a trimer. The 3×3 sub-blocks of the symmetrically equivalent chromophores contain only three different matrix elements each. The zero blocks are due to the neglect of transfer between non-neighboring trimers. The zeros in the last row and column indicate that back-transfer from the core to the rod and rod $\rightarrow$ core transfer from trimers not directly attached to the core are all neglected. The structure of the kinetic matrix is visualized in the scheme given on page 681 for a rod made up of three timers: The structure of the 3×3 sub-blocks is very simple. Two cases have to be considered: diagonal and off-diagonal sub-blocks.

The elements of the diagonal sub-blocks are

$$\begin{matrix} s & k & k \\ k & s & k \\ k & k & s, \end{matrix}$$

where k is the rate constant for transfers between the symmetrically equivalent chromophores, and s is the negative sum of all processes depleting the corresponding chromophore. (Note that according to this definition $s + 2k$ is independent of k [see below].)

The off-diagnonal sub-blocks also reflect the threefold symmetry of the rods.

$$\begin{matrix} k^0 & k^- & k^+ \\ k^+ & k^0 & k^- \\ k^- & k^+ & k^0. \end{matrix}$$

The superscripts ^{0}, $^-$, and $^+$ denote transfer to the three symmetrically equivalent accepting chromophores. Note that k, s, k^0, k^-, and k^+ values in different sub-blocks are different.

Making use of the assumed C_3 symmetry of the rods, the kinetic matrix may be split into several non-interacting blocks, i.e., blocks with no

	Trimer 1									Trimer 2									Trimer 3									
	S	S	S	M	M	M	F	F	F	S	S	S	M	M	M	F	F	F	S	S	S	M	M	M	F	F	F	APC
S	*	*	*	*	*	*	*	*	*	*	*	*	*	*	*	*	*	*	0	0	0	0	0	0	0	0	0	0
S	*	*	*	*	*	*	*	*	*	*	*	*	*	*	*	*	*	*	0	0	0	0	0	0	0	0	0	0
S	*	*	*	*	*	*	*	*	*	*	*	*	*	*	*	*	*	*	0	0	0	0	0	0	0	0	0	0
M	*	*	*	*	*	*	*	*	*	*	*	*	*	*	*	*	*	*	0	0	0	0	0	0	0	0	0	0
M	*	*	*	*	*	*	*	*	*	*	*	*	*	*	*	*	*	*	0	0	0	0	0	0	0	0	0	0
M	*	*	*	*	*	*	*	*	*	*	*	*	*	*	*	*	*	*	0	0	0	0	0	0	0	0	0	0
F	*	*	*	*	*	*	*	*	*	*	*	*	*	*	*	*	*	*	0	0	0	0	0	0	0	0	0	0
F	*	*	*	*	*	*	*	*	*	*	*	*	*	*	*	*	*	*	0	0	0	0	0	0	0	0	0	0
F	*	*	*	*	*	*	*	*	*	*	*	*	*	*	*	*	*	*	0	0	0	0	0	0	0	0	0	0
S	*	*	*	*	*	*	*	*	*	*	*	*	*	*	*	*	*	*	*	*	*	*	*	*	*	*	*	0
S	*	*	*	*	*	*	*	*	*	*	*	*	*	*	*	*	*	*	*	*	*	*	*	*	*	*	*	0
S	*	*	*	*	*	*	*	*	*	*	*	*	*	*	*	*	*	*	*	*	*	*	*	*	*	*	*	0
M	*	*	*	*	*	*	*	*	*	*	*	*	*	*	*	*	*	*	*	*	*	*	*	*	*	*	*	0
M	*	*	*	*	*	*	*	*	*	*	*	*	*	*	*	*	*	*	*	*	*	*	*	*	*	*	*	0
M	*	*	*	*	*	*	*	*	*	*	*	*	*	*	*	*	*	*	*	*	*	*	*	*	*	*	*	0
F	*	*	*	*	*	*	*	*	*	*	*	*	*	*	*	*	*	*	*	*	*	*	*	*	*	*	*	0
F	*	*	*	*	*	*	*	*	*	*	*	*	*	*	*	*	*	*	*	*	*	*	*	*	*	*	*	0
F	*	*	*	*	*	*	*	*	*	*	*	*	*	*	*	*	*	*	*	*	*	*	*	*	*	*	*	0
S	0	0	0	0	0	0	0	0	0	*	*	*	*	*	*	*	*	*	*	*	*	*	*	*	*	*	*	0
S	0	0	0	0	0	0	0	0	0	*	*	*	*	*	*	*	*	*	*	*	*	*	*	*	*	*	*	0
S	0	0	0	0	0	0	0	0	0	*	*	*	*	*	*	*	*	*	*	*	*	*	*	*	*	*	*	0
M	0	0	0	0	0	0	0	0	0	*	*	*	*	*	*	*	*	*	*	*	*	*	*	*	*	*	*	0
M	0	0	0	0	0	0	0	0	0	*	*	*	*	*	*	*	*	*	*	*	*	*	*	*	*	*	*	0
M	0	0	0	0	0	0	0	0	0	*	*	*	*	*	*	*	*	*	*	*	*	*	*	*	*	*	*	0
F	0	0	0	0	0	0	0	0	0	*	*	*	*	*	*	*	*	*	*	*	*	*	*	*	*	*	*	0
F	0	0	0	0	0	0	0	0	0	*	*	*	*	*	*	*	*	*	*	*	*	*	*	*	*	*	*	0
F	0	0	0	0	0	0	0	0	0	*	*	*	*	*	*	*	*	*	*	*	*	*	*	*	*	*	*	0
APC	0	0	0	0	0	0	0	0	0	0	0	0	0	0	0	0	0	0	*	*	*	*	*	*	*	*	*	*

non-zero off-diagonal elements in common. This is done using a symmetry adapted concentration vector $\mathbf{X}'$, which is related to $\mathbf{X}$ by

$$\mathbf{X}' = C\mathbf{X}.$$

K then transforms according to

$$K' = CKC^{-1}.$$

The transformation matrix may be obtained directly from the character table of the rotation group formed by the symmetrically equivalent chromophores.

Energy transfer among symmetrically equivalent chromophores can be observed only by polarization experiments. As long as one deals with unpolarized (isotropic) measurements, the symmetrically equivalent chromophores are indistinguishable. In this case only the temporal evolution of ΣX_{mn} (where the summation is over all symmetrically equivalent chromophores) is of interest, rather than the kinetics of individual chromophores. This sum actually corresponds to the totally symmetric combination of X_{mn}, since it is invariant under any permutation between the variables X_{mn}. (For a detailed discussion of group theoretical methods to simplify the structure of matrices see, e.g., reference 54.) Therefore only these parts of $\mathbf{X}'$ and K' (denoted as $\mathbf{X}'_{ts}$ and K'_{ts}, respectively) have to be considered in the calculation.

As an example, the transformation taking into account only the threefold symmetry axis of the rods is carried out below. In this case the elements of the transformation matrix C are zero except for the one in the lower left corner, which is 1, and for those in the 3×3 sub-blocks along the diagonal, which are obtained from the character table of the symmetry group C3. (Note that linear combinations within the two-dimensional E-representation have been formed):

$$\begin{matrix} 1 & 1 & 1 \\ 2 & -1 & -1 \\ 0 & 1 & -1. \end{matrix}$$

The diagonal sub-blocks in K' then become

$$\begin{matrix} s+2k & 0 & 0 \\ 0 & s-k & 0 \\ 0 & 0 & s-k, \end{matrix}$$

and the off-diagonal sub-blocks

$$\begin{matrix} k^0+k^-+k^+ & 0 & 0 \\ 0 & k^0-(k^-/2)-(k^+/2) & (3k^-/2)-(3k^+/2) \\ 0 & (k^+/2)-(k^-/2) & k^0-(k^-/2)-(k^+/2). \end{matrix}$$

The first rows and columns of these sub-blocks belong to the totally symmetric part of K'. In the last row of K' the elements in the nontotally symmetric part vanish, whereas those in the totally symmetric part are the same as in K. The $(3N+1, 3N+1)$ element in the lower right corner also remains unchanged. Thus the dimension of the relevant kinetic matrix K'_{ts} is only $3 \times N + 1$.

In the case of $N = 3$, K'_{ts} has the following structure:

*	*	*	*	*	*	0	0	0	0
*	*	*	*	*	*	0	0	0	0
*	*	*	*	*	*	0	0	0	0
*	*	*	*	*	*	*	*	*	0
*	*	*	*	*	*	*	*	*	0
*	*	*	*	*	*	*	*	*	0
0	0	0	*	*	*	*	*	*	0
0	0	0	*	*	*	*	*	*	0
0	0	0	*	*	*	*	*	*	0
0	0	0	0	0	0	*	*	*	*.

An asterisk denotes a non-zero element. In model A, where all C-PC chromophores in a trimer are considered to be symmetrically equivalent, the dimension of K'_{ij} may be reduced to $N + 1$.

APPENDIX B

Detailed Kinetic Matrix for the Model Shown in Fig. 5

$$\begin{array}{cccccccccc}
\alpha & 0 & 0 & f \cdot k_{RR} & 0 & 0 & 0 & 0 & 0 & 0 \\
k_{SM} & \beta & k_{FM} & 0 & f \cdot k_{RR} & 0 & 0 & 0 & 0 & 0 \\
k_{SF} & k_{MF} & \kappa & 0 & 0 & f \cdot k_{RR} & 0 & 0 & 0 & 0 \\
k_{RR} & 0 & 0 & \delta & 0 & 0 & f \cdot k_{RR} & 0 & 0 & 0 \\
0 & k_{RR} & 0 & k_{SM} & \epsilon & k_{FM} & 0 & f \cdot k_{RR} & 0 & 0 \\
0 & 0 & k_{RR} & k_{SF} & k_{MF} & \rho & 0 & 0 & f \cdot k_{RR} & 0 \\
0 & 0 & 0 & k_{RR} & 0 & 0 & \gamma & 0 & 0 & 0 \\
0 & 0 & 0 & 0 & k_{RR} & 0 & k_{SM} & \eta & k_{FM} & 0 \\
0 & 0 & 0 & 0 & 0 & k_{RR} & k_{SF} & k_{MF} & \mu & 0 \\
0 & 0 & 0 & 0 & 0 & 0 & k_{RC} & k_{RC} & k_{RC} & -1/\tau_{APC}
\end{array}$$

The symbols α–μ in the matrix are given by

$$\alpha = -1/\tau_{PC} - k_{SM} - k_{SF} - k_{RR}$$

$$\beta = -1/\tau_{PC} - k_{MF} - k_{RR}$$

$$\kappa = -1/\tau_{PC} - k_{FM} - k_{RR}$$

$$\delta = -1/\tau_{PC} - k_{SM} - k_{SR} - (1 + f)\, k_{RR} = \alpha - f \cdot k_{RR}$$

$$\epsilon = -1/\tau_{PC} - k_{MF} - (1 + f)\, k_{RR} = \beta - f \cdot k_{RR}$$

$$\rho = -1/\tau_{PC} - k_{FM} - (1 + f)\, k_{RR} = \kappa - f \cdot k_{RR}$$

$$\gamma = -1/\tau_{PC} - k_{SM} - k_{SF} - k_{RR} - k_{RC} = \alpha - k_{RC}$$

$$\eta = -1/\tau_{PC} - k_{MF} - k_{RR} - k_{RC} = \beta - k_{RC}$$

$$\mu = -1/\tau_{PC} - k_{FM} - k_{RR} - k_{RC} = \kappa - k_{RC}.$$

We thank Professor K. Sauer for critically reading the manuscript and Professor K. Schaffner for his interest and support of this work.

Received for publication 12 May 1987 and in final form 9 July 1987.

REFERENCES

1. Wildman, R. B., and C. C. Bowen. 1974. Phycobilisomes in blue-green algae. *J. Bacteriol.* 117:866–881.
2. Koller, K. P., and W. Wehrmeyer. 1974. Isolation and characterization of the biliproteins from Rhodella violacea (Bangiophycidae). *Arch. Microbiol.* 100:253–270.
3. Wehrmeyer, W. 1983. Organization and composition of cyanobacterial and rhodophycean phycobilisomes. *In* Photosynthetic Prokaryotes. G. C. Papageorgiou and L. Packer, editors. Elsevier, Amsterdam, New York. 1–22.
4. Bryant, D. A., G. Guglielmi, N. Tandeau de Marsac, A.-M. Castets, and G. Cohen-Bazire. 1979. The structure of cyanobacterial phycobilisomes: a model. *Arch. Microbiol.* 123:113–127.
5. Gantt, E. 1980. Structure and function of phycobilisomes: light harvesting pigment complexes in red and blue-green algae. *Int. Rev. Cytol.* 66:45–80.
6. Zuber, H. 1978. Studies on the structure of the light-harvesting pigment-protein complexes from cyanobacteria and red algae. *Ber. Dtsch. Bot. Ges.* 91:459–475.
7. Koller, K. P., W. Wehrmeyer, and H. Schneider. 1977. Isolation and characterization of disc-shaped phycobilisomes from the red alga Rhodella violacea. *Arch. Microbiol.* 112:61–67.
8. Nies, M., and W. Wehrmeyer. 1980. Isolation and biliprotein characterization of phycobilisomes from the thermophilic cyanobacterium Mastigocladus laminosus Cohn. *Planta.* 150:330–337.
9. Glazer, A. N. 1982. Phycobilisomes: structure and dynamics. *Annu. Rev. Microbiol.* 36:173–198.
10. Mörschel, E., and K. Mühlethaler. 1983. On the linkage of exoplasmatic freeze-facture particles to phycobilisomes. *Planta.* 158:451–457.
11. Scheer, H. 1982. Phycobiliproteins: molecular aspects of a photosynthetic antenna system. *Mol. Biol Biochem. Biophys.* 35:7–45.
12. Gantt, E. 1981. Phycobilisomes. *Annu. Rev. Plant Physiol.* 32:327–347.
13. Glazer, A. N., D. J. Lundell, G. Yamanaka, and R. C. Williams. 1983. The structure of a simple phycobilisome. *Ann. Microbiol.* 134B:159–180.
14. Clement-Metral, J.D., and E. Gantt. 1983. Isolation of oxygen-evolving phycobilisome-photosystem II particles from Porphyridium cruentum. *FEBS (Fed. Eur. Biochem. Soc.) Lett.* 156:185–188.
15. Schatz, G. H., and H. T. Witt. 1984. Extraction and characterization of oxygen-evolving photosystem II complexes from a thermophilic cyanobacterium Synechococcus spec. *Photobiochem. Photobiophys.* 7:1–14.
16. Scheer, H. 1986. Excitation transfer in phycobiliproteins. *In* Encyclopedia of Plant Physiology: Photosynthesis III. Vol. 19. L. A. Staehelin and C. J. Arntzen, editors. Springer-Verlag, Berlin, Heidelberg, 327–337.
17. Karukstis, K. K., and K. Sauer. 1983. Fluorescence decay kinetics of chlorophyll in photosynthetic membranes. *J. Cell Biochem.* 23:131–158.
18. Holzwarth, A. R. 1986. Fluorescence lifetimes in photosynthetic systems. *Photochem. Photobiol.* 43:707–725.
19. Holzwarth, A. R., J. Wendler, and W. Wehrmeyer. 1983. Studies on chromophore coupling in isolated phycobiliproteins. I. Picosecond fluorescence kinetics of energy transfer in phycocyanin 645 from Chroomonas sp. *Biochim. Biophys. Acta.* 724:388–395.
20. Suter, G. W., P. Mazzola, J. Wendler, and A. R. Holzwarth. 1984. Fluorescence decay kinetics in phycobilisomes from the blue-green alga Synechococcus 6301. *Biochim. Biophys. Acta.* 766:269–276.
21. Wendler, J., A. R. Holzwarth, and W. Wehrmeyer. 1984. Picosecond time-resolved energy transfer in phycobilisomes isolated from the red alga Porphyridium cruentum. *Biochim. Biophys. Acta.* 765:58–67.
22. Wehrmeyer, W., J. Wendler, and A. R. Holzwarth. 1985. Biochemical and functional characterization of a peripheral unit of the phycobilisomes from Porphyridium cruentum. Measurement of picosecond energy transfer kinetics. *Eur. J. Cell Biol.* 36:17–23.
23. Gillbro, T., A. Sandström, V. Sundström, J. Wendler, and A. R. Holzwarth. 1985. Picosecond study of energy transfer kinetics in physobilisomes of Synechococcus 6301 and the mutant AN 112. *Biochim. Biophys. Acta.* 808:52–65.
24. Holzwarth, A. R., J. Wendler, and G. W. Suter. 1987. Studies on chromophore coupling in isolated phycobiliproteins. II. Picosecond energy transfer kinetics and time-resolved fluorescence spectra of C-Phycocyanin from Synechococcus 6301 as a function of the aggregation state. *Biophys. J.* 51:1–12.
25. Wendler, J., W. John, H. Scheer, and A. R. Holzwarth. 1986. Energy transfer kinetics in trimeric C-phycocyanin studied by picosecond fluorescence kinetics. *Photochem. Photobiol.* 44:79–85.
26. Hefferle, P., W. John, H. Scheer, and S. Schneider. 1984. Thermal denaturation of monomeric and trimeric phycocyanins studied by static and polarized time-resolved fluorescence spectroscopy. *Photochem. Photobiol.* 39:221–232.
27. Hefferle, P., P. Geiselhart, T. Mindl, S. Schneider, W. John, and H. Scheer. 1984. Time-resolved polarized fluorescence of C-phycocyanin and its subunits from Mastigocladus laminosus. *Z. Naturforsch. Sect. C. Biosci.* 39c:606–616.

28. Hefferle, P., M. Nies, W. Wehrmeyer, and S. Schneider. 1983. Picosecond time-resolved fluorescence study of the antenna system isolated from Mastigocladus laminosus Cohn. I. Functionally intact phycobilisomes. *Photobiochem. Photobiophys.* 5:41–51.
29. Hefferle, P., M. Nies, W. Wehrmeyer, and S. Schneider. 1983. Picosecond time-resolved fluorescence study of the antenna system isolated from Mastigocladus laminosus Cohn. II. Constituent biliproteins in various forms of aggregation. *Photobiochem. Photobiophys.* 5:325–334.
30. Gillbro, T., A. Sandström, V. Sundström, and A. R. Holzwarth. 1983. Polarized absorption picosecond kinetics as a probe of energy transfer in phycobilisomes of Synechococcus 6301 *FEBS (Fed. Eur. Biochem. Soc.) Lett.* 162:64–68.
31. Schirmer, T., W. Bode, R. Huber, W. Sidler, and H. Zuber. 1985. X-ray crystallographic structure of the light-harvesting biliprotein C-phycocyanin from the thermophilic cyanobacterium Mastigocladus laminosus and its resemblance to globin structures. *J. Mol. Biol.* 184:257–277.
32. Sauer, K., and H. Scheer. 1987. Excitation transfer rates in c-phycocyanin Förster transfer calculations based on crystal structure data from Agmenellum quadruplicatum c-phycocyanin. *Photochem. Photobiol.* 1–49.
33. Scheer, H., 1987. Photochemistry and photophysics of c-phycocyanin. *In* Progress in Photosynthesis Research. Vol. 1. J. Biggins, editor. Nijhoff, Dordrecht. 143–149.
34. Sauer, K. 1987. Fluorescence decay and depolarization kinetics calculated using Förster inductive resonance and the molecular coordinates for c-phycocyanin. *In* Progress in Photosynthesis Research. Vol. 1. J. Biggins, editor. Nijhoff, Dordrecht. 139–142.
35. Porter, G., C. J. Tredwell, G. F. W. Searle, and J. Barber. 1978. Picosecond time-resolved energy transfer in Porphyridium cruentum. Part I. In the intact alga. *Biochim. Biophys. Acta.* 501:232–245.
36. Yamazaki, I., M. Mimuro, T. Murao, T. Yamazaki, K. Yoshihara, and Y. Fujita. 1984. Excitation energy transfer in the light harvesting antenna system of the red alga Porphyridium cruentum and the blue-green alga Anacystis nidulans: analysis of time-resolved fluorescence spectra. *Photochem. Photobiol.* 39:233–240.
37. Holzwarth, A. R. 1985. Energy transfer kinetics in phycobilisomes *In* Antennas and Reaction Centers of Photosynthetic Bacteria. M. E. Michel-Beyerle, editors. Springer-Verlag, Berlin. 45–52.
38. Glazer, A. N., C. Chan, R. C. Williams, S. W. Yeh, and J. H. Clark. 1985. Kinetics of energy flow in the phycobilisome core. *Science (Wash. DC).* 230:1051–1053.
39. Holzwarth, A. R., J. Wendler, and W. Wehrmeyer. 1982. Picosecond time resolved energy transfer in isolated phycobilisomes from Rhodella violacea (Rhodophyceae). *Photochem. Photobiol.* 36:479–487.
40. Förster, T. 1948. Intermolecular energy transfer and fluorescence. *Ann. Phys. Leipzig.* 2:55–75.
41. Förster, T. 1949. Experimentelle und theoretische Untersuchung des zwischenmolekularen Uebergangs von Elektronenanregungsenergie. *Z. Naturforsch. Sect. C. Biosci.* 4A:321–327.
42. Schirmer, T., R. Huber, M. Schneider, W. Bode, M. Miller, and M. L. Hackert. 1986. Crystal structure analysis and refinement at 2.5 A of hexameric c-phycocyanin from the cyanobacterium Agmenellum quadruplicatum. The molecular model and its implications for light harvesting. *J. Mol. Biol.* 188:651–676.
43. Grabowski, J., and E. Gantt. 1978. Photophysical properties of phycobiliproteins from phycobilisomes: fluorescence lifetimes, quantum yield, and polarization spectra. *Photochem. Photobiol.* 28:39–45.
44. Seibert, M., and J. C. Connolly. 1984. Fluorescence properties of c-phycocyanin isolated from a thermophilic cyanobacterium. *Photochem. Photobiol.* 40:267–271.
45. Dale, R. E., and F. W. J. Teale. 1970. Number and distribution of chromophore types in native phycobiliproteins. *Photochem. Photobiol.* 12:99–117.
46. Mimuro, M., P. Füglistaller, R. Rümbeli, and H. Zuber. 1986. Functional assignment of chromophores and energy transfer in C-phycocyanin isolated from the thermophilic cyanobacterium Mastigocladus laminosus. *Biochim. Biophys. Acta.* 848:155–166.
47. Pearlstein, R. M. 1982. Exciton migration and trapping in photosynthesis. *Photochem. Photobiol.* 35:835–844.
48. Pearlstein, R. M. 1967. Migration and trapping of excitation quanta in photosynthetic units. *Brookhaven Symp. Biol.* 19:8–15.
49. Montroll, E. W. 1969. Random walks on lattices. III. Calculation of first-passage times with application to exciton trapping on photosynthetic units. *J. Math. Phys.* 10:753–765.
50. Glazer, A. N., S. W. Yeh, S. P. Webb, and J. H. Clark. 1985. Disk-to-disk transfer as the rate-limiting step for energy flow in phycobilisomes. *Science (Wash. DC).* 227:419–423.
51. Grabowski, J., and E. Gantt. 1978. Excitation energy migration in phycobilisomes: comparison of experimental results and theoretical predictions. *Photochem. Photobiol.* 28:47–54.
52. Searle, G. F. W., J. Barber, G. Porter, and C. J. Tredwell. 1978. Picosecond time-resolved energy transfer in Porphyridium cruentum. Part II. In the isolated light harvesting complex (phycobilisomes). *Biochim. Biophys. Acta.* 501:246–256.
53. Mimuro, M., I. Yamazaki, T. Murao, K. Yoshihara, and Y. Fujita. 1984. Excitation energy transfer in phycobilin-chlorophyll a system in blue-green and red algae. *Adv. Photosyn. Res.* 1:21–28.
54. Cotton, F. A. 1963. Chemical Application of Group Theory. John Wiley & Sons, Inc., New York.